Electronic Supplementary Material (ESI) for Dalton Transactions.

Electronic Supplementary Information
(ESI)

Anion-Directed Supramolecular Chemistry Modulating the Magnetic Properties of Nanoscopic Mn Coordination Clusters: From Polynuclear High-Spin Complexes to SMMs

Lei Zhang,[a,b] *Theresa Chimamkpam,*[b] *Camelia I. Onet,*[b] *Nianyong Zhu,*[b,c] *Rodolphe Clérac,*[d,e] *and Wolfgang Schmitt**[b]

[a] State Key Laboratory of Structural Chemistry, Fujian Institute of Research on the Structure of Matter, Chinese Academy of Sciences, Fuzhou, Fujian 350002, P. R. China
[b] School of Chemistry & CRANN, University of Dublin, Trinity College, Dublin 2, Ireland.
[c] Institute of Molecular Functional Materials & Department of Chemistry, Hong Kong Baptist University, Waterloo Road, Hong Kong, HK
[d] CNRS, CRPP, UPR 8641, Pessac F-33600, France.
[e] Univ. Bordeaux, CRPP, UPR 8641, F-33600 Pessac, France

E-mail: schmittw@tcd.ie

Experimental Section

Materials and Instrumentation. Commercially available reagents were bought from Sigma-Aldrich or ABCR and used as received without further purification. Fourier transform infrared spectroscopy (FTIR) data were collected on a Perkin-Elmer Spectrum 100 FT-IR Spectrometer. Elemental analyses (C, H, and N) were obtained from Microanalysis Lab, School of Chemistry & Chemical Biology, University College Dublin. The magnetic susceptibility measurements were obtained with the use of MPMS-XL Quantum Design SQUID magnetometer and PPMS-9 susceptometer. These magnetometer and susceptometer work between 1.8 and 400 K for dc applied fields ranging from -7 to 7 T (MPMS-XL). Measurements were performed on using polycrystalline samples (*ca.* 8-15 mg). Instantly prior to the measurements, the coordination compounds were separated from the mother liquor, dried for a few minutes at room temperature and sealed in polyethylene bags (3 cm × 0.5 cm × 0.02 cm; typically 15 to 30 mg) and covered by mineral oil (typical 3 to 8 mg) to avoid torquing effects. ac susceptibility measurements were measured with an oscillating ac field of 1 to 6 Oe with frequency between 10 to 10000 Hz (PPMS). The magnetic data were corrected for the sample holder, mineral oil and the diamagnetic contribution.

Preparation of reaction mixture that led to the co-crystallization of I, II, and III: A mixture of $MnCl_2 \cdot 4H_2O$ (0.295 g, 1.5 mmol), $KMnO_4$ (0.031 g, 0.2 mmol), *tert*-butylphosphonic acid (0.137 g, 1.0 mmol), pyridine (0.12 ml) and CH_3CN (25 mL) was stirred at room temperature for 5 hours and then filtered. The filtrate was kept at room temperature and large amount of red crystals were obtained after several weeks, from which complexes of **I**, **II**, and **III** were characterized.

Synthesis of III: Pure red crystals of **III** can be obtained by similar reaction as described above, but increasing the amount of $MnCl_2 \cdot 4H_2O$ to 0.396 g (2.0 mmol). Yield: 60 % (based on Mn). CHN analysis on dried sample, expected for $Mn_{21}P_{18}O_{66}N_8C_{112}H_{209}Cl_7$ (corresponding to the crystal formula and a loss of 1 CH_3CN): calcd. (found) C 28.72 (27.56), H 4.50 (4.33), N 2.39 (2.16)%.

Synthesis of IV: A mixture of $MnCl_2 \cdot 4H_2O$ (0.201 g, 1.0 mmol), $KMnO_4$ (0.016 g, 0.1 mmol), *tert*-butylphosphonic acid (0.136 g, 1.0 mmol), 2-amino-pyridine (0.189 g, 2.0 mmol) and CH_3OH

(20 mL) was stirred at room temperature for 5 hours and then filtered. The filtrate was kept at room temperature, and red crystals of **IV** were obtained within one week. Yield: 65 % (based on Mn). CHN analysis on dried sample, expected for $Mn_{15}P_{12}Cl_2O_{58}C_{64}N_4H_{160}$ (corresponding to the crystal formula and a loss of 3 CH_3OH): calcd. (found) C 24.17 (24.42), H 5.07 (4.24), N 1.76 (1.61)%.

X-ray Crystallography. Single crystal X-ray structure determination of the five compounds, $[Mn^{III}_6$(*tert*-butyl-$PO_3)_8$(pyridine)$_6$(Cl)]$_2[Mn^{II}_3Mn^{III}_9(\mu_4\text{-}O)_6(\mu_3\text{-}OH)_2(\mu_4\text{-}Cl)_4$(*tert*-butyl-$PO_3H)_3$-(*tert*-butyl-$PO_3)_7]\cdot 2.5H_2O\cdot 6CH_3CN$ (**I**, include **$Mn_{12}P_{10}\subset Cl_4$**), $[Mn^{III}_6$(*tert*-butyl-$PO_3)_8$-(pyridine)$_6$(Cl)]$[Mn^{II}_2Mn^{III}_{11}(\mu_4\text{-}O)_6(\mu_3\text{-}O)(\mu_3\text{-}OH)(\mu_4\text{-}Cl)_4$(*tert*-butyl-$PO_3H$)(*tert*-butyl-$PO_3)_9$-$(H_2O)]\cdot 2H_2O\cdot 9CH_3CN$ (**II**, include **$Mn_{13}P_{10}\subset Cl_4$**), $[Cl\subset Mn^{III}_6$ (*tert*-butyl-$PO_3)_8$(pyridine)$_6$]-$[Mn^{II}_3Mn^{III}_{12}(\mu_4\text{-}O)_6(\mu_3\text{-}O)_2(\mu_3\text{-}OH)(\mu_4\text{-}Cl)_4(Cl)_2$(*tert*-butyl-$PO_3)_{10}(H_2O)$(pyridine)$_2]\cdot 2H_2O$-$\cdot CH_3CN$ (**III**, include **$Mn_{15}P_{10}\subset Cl_4$**), and (2-amino-Hpyridine)$_2[Mn^{II}_3Mn^{III}_{12}(\mu_4\text{-}O)_8(\mu_4\text{-}Cl)_2$-$(\mu\text{-}CH_3O)_4(CH_3OH)_2$(*tert*-butyl-$PO_3H)_2$(*tert*-butyl-$PO_3)_{10}]\cdot 8H_2O\cdot 3CH_3OH$ (**IV**) was performed at 150(K) on the Bruker SMART Apex diffractometer using graphite-monochromated Mo-Kα radiation. Absorption corrections were applied using SADABS.[1] Structures were solved by direct method and refined by full-matrix least-squares on F^2 using *SHELXTL*.[2] Contributions to scattering due to disordered solvent molecules were removed using the *SQUEEZE* routine of *PLATON*;[3] structures were then refined again using the data generated. Crystal data and details of data collection and refinement of **I–IV** were summarized in Table S1. Crystallographic data, CCDC **1062487–1062490**, can be obtained free of charge from the Cambridge Crystallographic Data Centre *via*www.ccdc.cam.ac.uk/data_request/cif.

1. Sheldrick, G. M. *SADABS, Program for area detector adsorption correction*. Institute for Inorganic Chemistry, University of Göttingen, Göttingen (Germany), **1996**.
2. Sheldrick, G. M. *SHELXL-97, Program for solution of crystal structures*. University of Göttingen, Göttingen (Germany), **1997**.
3. Vandersluis, P.; Spek, A. L. *Acta Crystallogr.A* **1990**, *46*, 194.

Table S1. Crystal data and structure refinements for **I-IV**.

	I	**II**	**III**	**IV**
Crystal. det. formula	$Mn_{24}P_{26}O_{90}N_{20}C_{180}H_{330}Cl_6$	$Mn_{19}P_{18}O_{65}N_{18}C_{126}H_{232}Cl_5$	$Mn_{42}P_{36}O_{134}N_{36}C_{264}H_{476}Cl_{14}$	$Mn_{15}P_{12}O_{62}N_4C_{76}H_{190}Cl_2$
Mr	6551.10	4817.85	10213.70	3417.44
crystal system	orthorhombic	monoclinic	triclinic	monoclinic
space group	*Pnma*	$P2_1/c$	*P*-1	$P2_1/c$
a [Å]	42.075(8)	25.261(5)	15.503(3)	17.320(3)
b [Å]	46.492(9)	29.077(6)	23.446(5)	15.550(3)
c [Å]	14.649(3)	30.460(6)	33.878(7)	30.118(6)
α [°]	90.00	90.00	92.11(3)	90.00
β [°]	90.00	111.77(3)	95.61(3)	105.40(3)
γ [°]	90.00	90.00	108.02(3)	90.00
V [Å^3]	28656(10)	20778(7)	11625(4)	7820(3)
Z	4	4	1	2
T [K]	150	150	150	150
ρ_c [g cm^{-3}]	1.518	1.540	1.459	1.451
μ [mm^{-1}]	1.295	1.390	1.372	1.398
reflns coll.	164628	120476	129226	84934
unique reflns	25616	36656	42527	14423
GOF	1.037	1.114	1.052	1.032
$R1$ [$I>2\sigma(I)$][a]	0.0768	0.0984	0.0558	0.0616
$wR2$[$I>2\sigma(I)$][b]	0.1667	0.2015	0.1531	0.1459

[a] $R1 = \Sigma||F_o| - |F_c||/\Sigma|F_o|$. [b] $wR2 = \{\Sigma[w(F_o^2 - F_c^2)^2]/\Sigma[w(F_o^2)^2]\}^{1/2}$.

Table S2. Bond valance sum calculations for the polynuclear Mn-based complexes in **I–IV.**

I	**Mn site**	Mn1	Mn2	Mn3	Mn4	Mn5	Mn6	Mn7	Mn8	Mn9	Mn10	Mn11	Mn12	Mn13
	BVS	3.491	3.455	3.414	3.524	3.392	3.415	2.435	3.008	2.980	3.052	3.250	1.735	3.215
	assigned O.S.	+3	+3	+3	+3	+3	+3	+2	+3	+3	+3	+3	+2	+3
II	**Mn site**	Mn1	Mn2	Mn3	Mn4	Mn5	Mn6	Mn7	Mn8	Mn9	Mn10	Mn11	Mn12	Mn13
	BVS	3.347	3.401	3.327	3.392	3.458	3.407	2.563	2.975	2.870	3.194	3.092	3.174	1.720
	assigned O.S.	+3	+3	+3	+3	+3	+3	+2	+3	+3	+3	+3	+3	+2
	Mn site	Mn14	Mn15	Mn16	Mn17	Mn18	Mn19							
	BVS	3.065	3.168	3.163	3.093	2.940	2.951							
	assigned O.S.	+3	+3	+3	+3	+3	+3							
III	**Mn site**	Mn1	Mn2	Mn3	Mn4	Mn5	Mn6	Mn7	Mn8	Mn9	Mn10	Mn11	Mn12	Mn13
	BVS	3.205	3.193	3.183	3.212	3.185	3.221	1.841	1.749	3.023	3.078	1.727	3.113	3.154
	assigned O.S.	+3	+3	+3	+3	+3	+3	+2	+2	+3	+3	+2	+3	+3
	Mn site	Mn14	Mn15	Mn16	Mn17	Mn18	Mn19	Mn20	Mn21					
	BVS	3.106	3.037	3.198	2.979	3.107	2.923	3.085	3.181					
	assigned O.S.	+3	+3	+3	+3	+3	+3	+3	+3					
IV	**Mn site**	Mn1	Mn2	Mn3	Mn4	Mn5	Mn6	Mn7	Mn8					
	BVS	1.560	3.130	3.204	3.221	3.011	2.939	3.257	1.778					
	assigned O.S.	+2	+3	+3	+3	+3	+3	+3	+2					

(a)

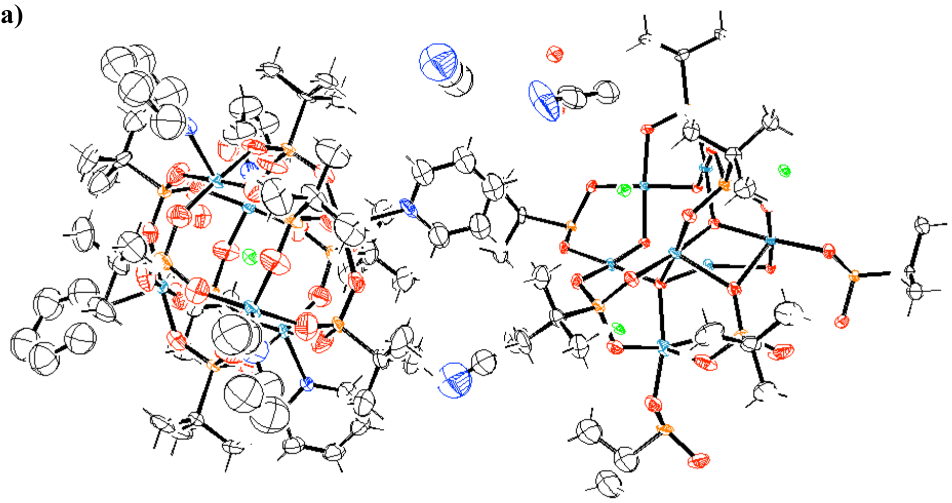

(b)

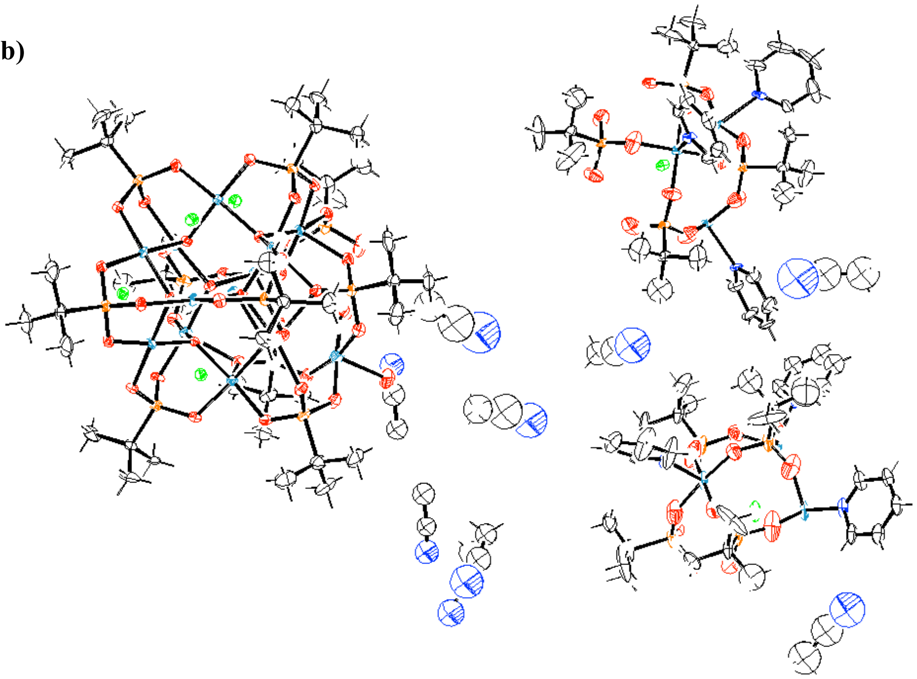

(c)

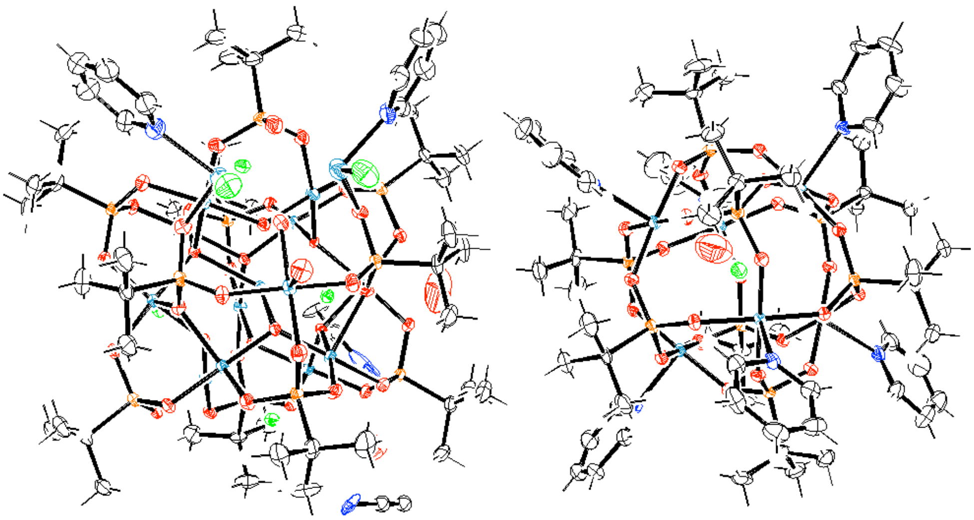

(d)

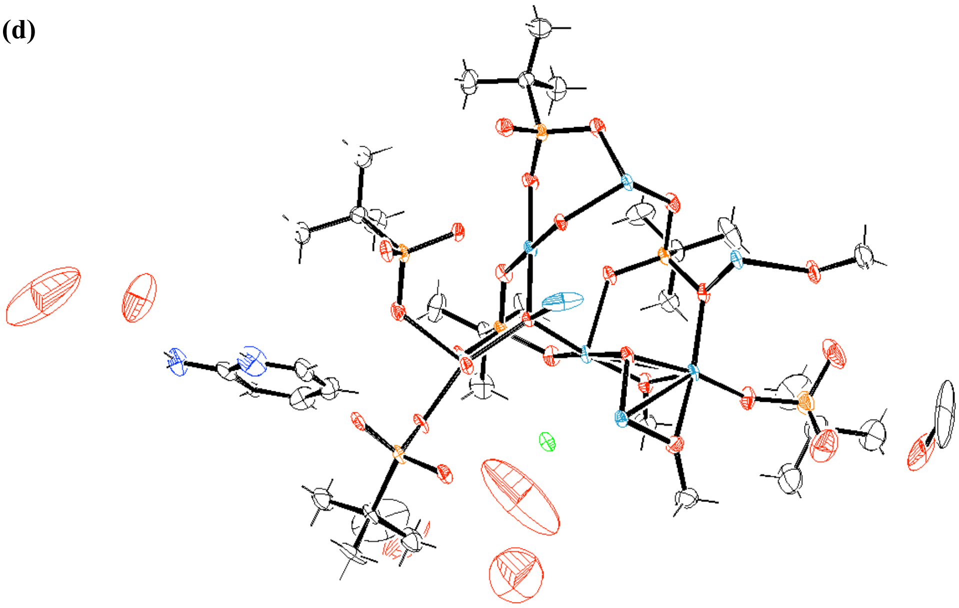

Fig. S1 Ortep diagrams for the asymmetric unit of (a) **I**; (b) **II**; (c) **III**; (d) **IV**. Ellipsoids shown at 50% probability, hydrogen atoms omitted for clarity. Color code: Mn sky blue, P orange, O red, C black, Cl green, N blue.

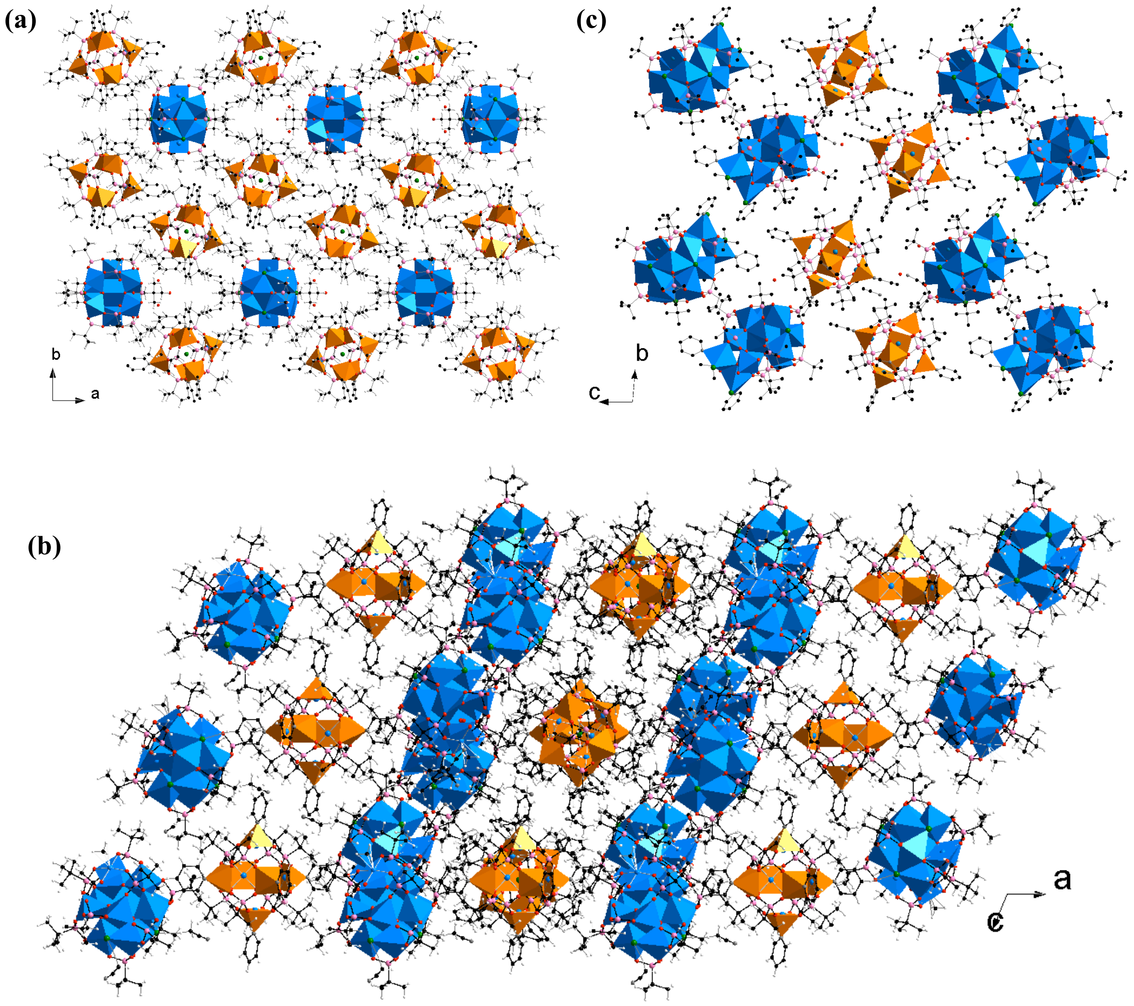

Fig. S2 Packing arrangement of the anionic Mn coordination clusters (blue polyhedra) and cationic Mn complexes (orange polyhedra) in (a) **I**; (b) **II**; (c) **III**.

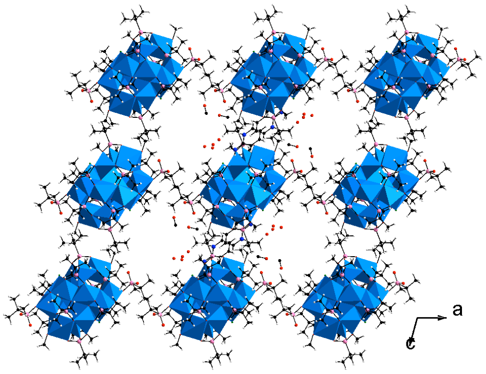

Fig. S3 Packing arrangement of the anionic Mn coordination clusters (blue polyhedra) in **IV**.

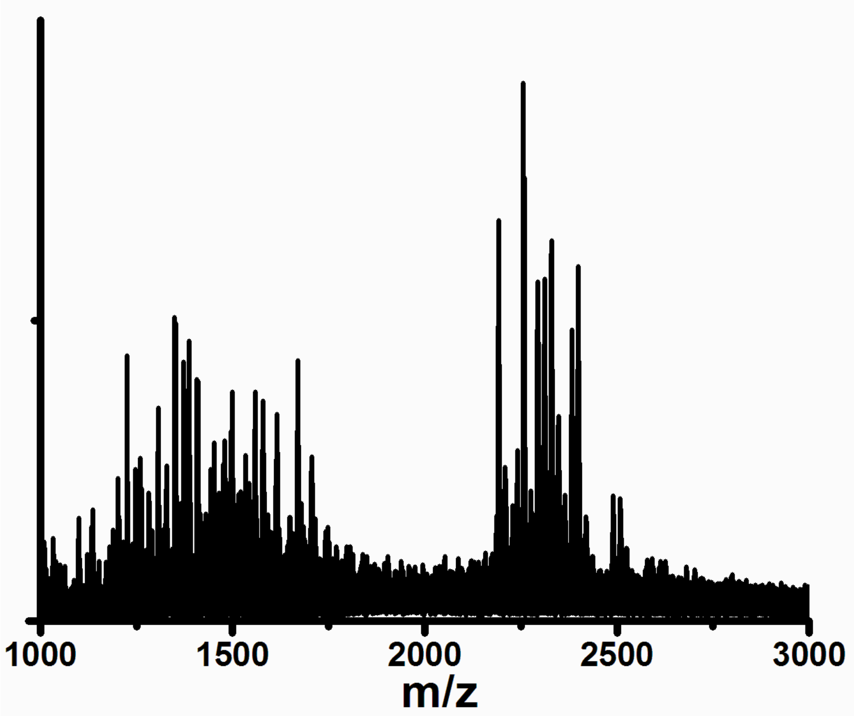

Fig. S4 Negative-mode MALDI-MS spectra to identify the co-crystallization of **I**, **II**, and **III** in the reaction mixture 24 hours after preparation.

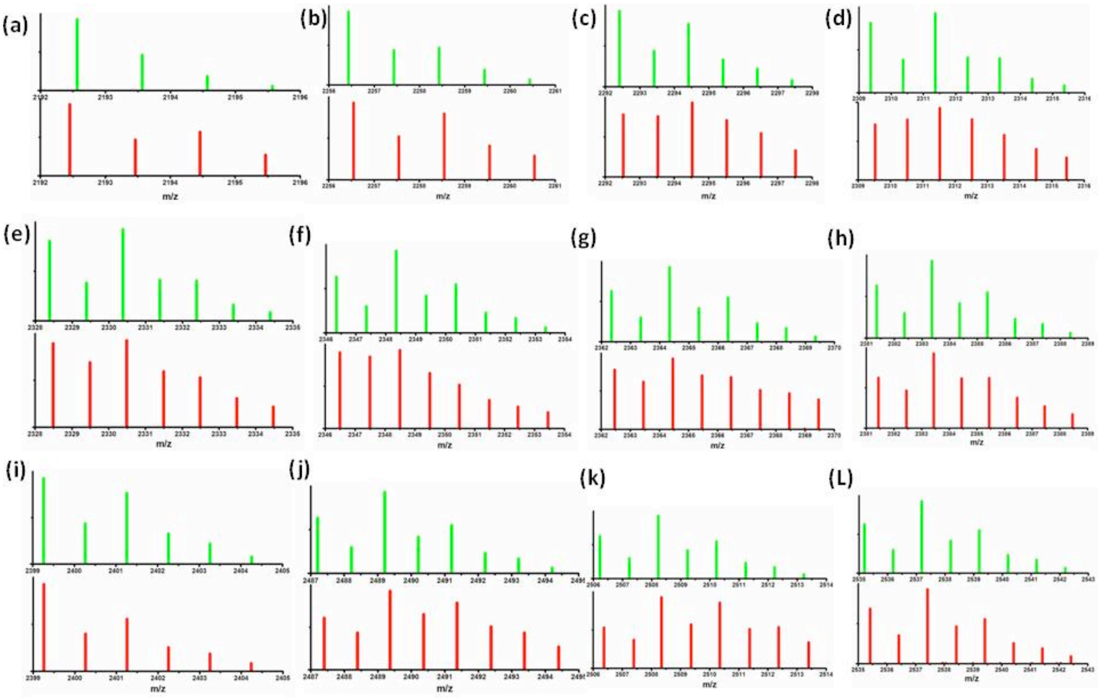

Fig. S5 Comparison of experimental isotopic envelops (red spectra) with simulated patterns (green spectra) for signals in Figure S4 and Table 1, *m/z*: (a) 2192.45; (b) 2256.55; (c) 2292.52; (d) 2311.53; (e) 2330.49; (f) 2348.49; (g) 2364.46; (h) 2383.44; (i) 2399.25; (j) 2489.36; (k) 2508.35; (l) 2537.41.

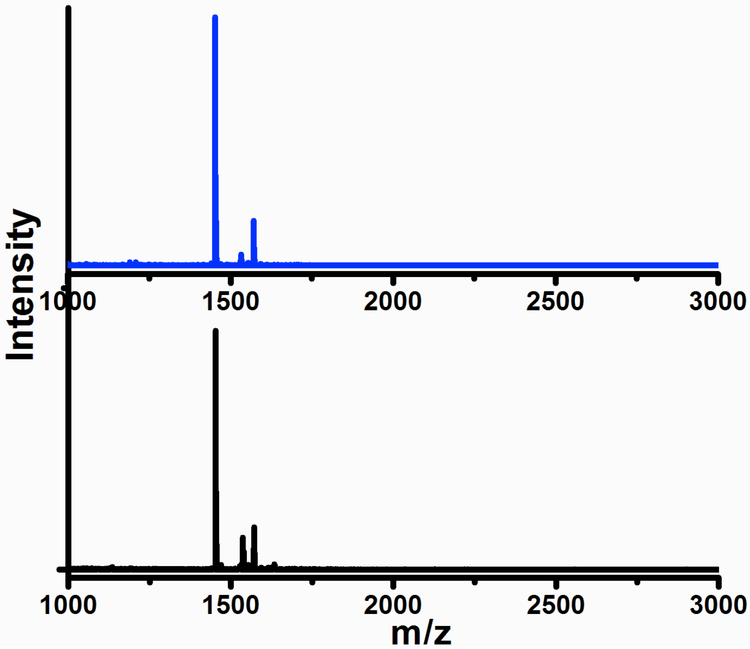

Fig. S6 Positive-mode MALDI-MS spectra to identify the charge-balancing [Cl⊂Mn$_6$(*tert*-butyl-PO$_3$)$_8$]$^+$ cluster in **I**, **II** and **III**: (upper) reaction mixture 24 hours after preparation; (bottom) crystalline products dissolved in CH$_3$CN. Signals centered at *m*/*z* 1452.81 correspond to [Cl⊂Mn$_6$(*tert*-butyl-PO$_3$)$_8$]$^+$ (calcd. *m*/*z* 1452.83).

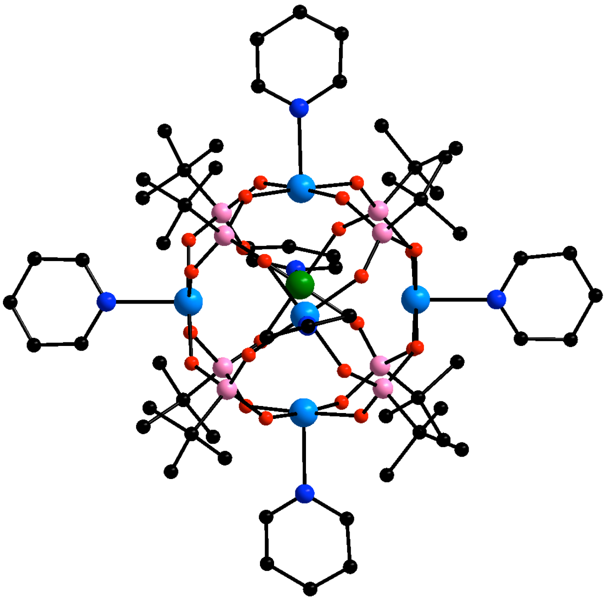

Fig. S7 Structure-type that forms as charge-balancing [Cl⊂Mn$_6$(*tert*-butyl-PO$_3$)$_8$]$^+$ coordination cluster in **I**, **II** and **III**; see also *Chem. Commun.* **2013**, 66.

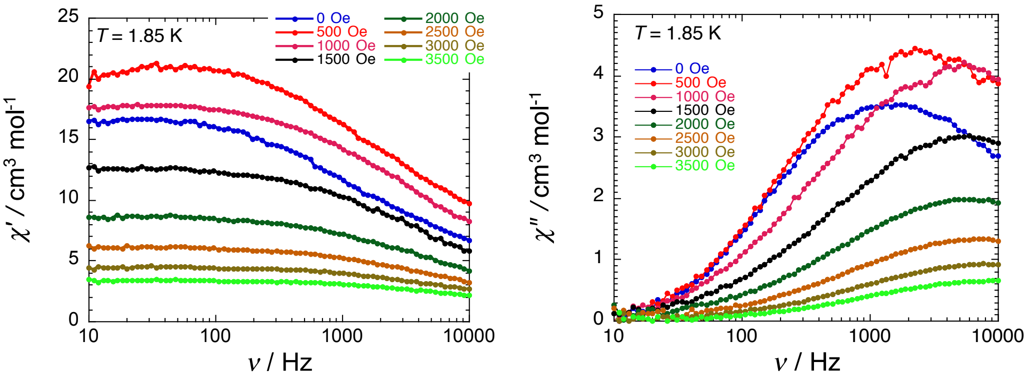

Fig. S8 Frequency dependence of the real (χ', left) and imaginary (χ'', right) components of the ac susceptibility, between 0 and 3500 Oe and between 10 and 10000 Hz, for **$Mn_{15}P_{12}\subset Cl_2$** at 1.85 K. Solid lines are visual guides.

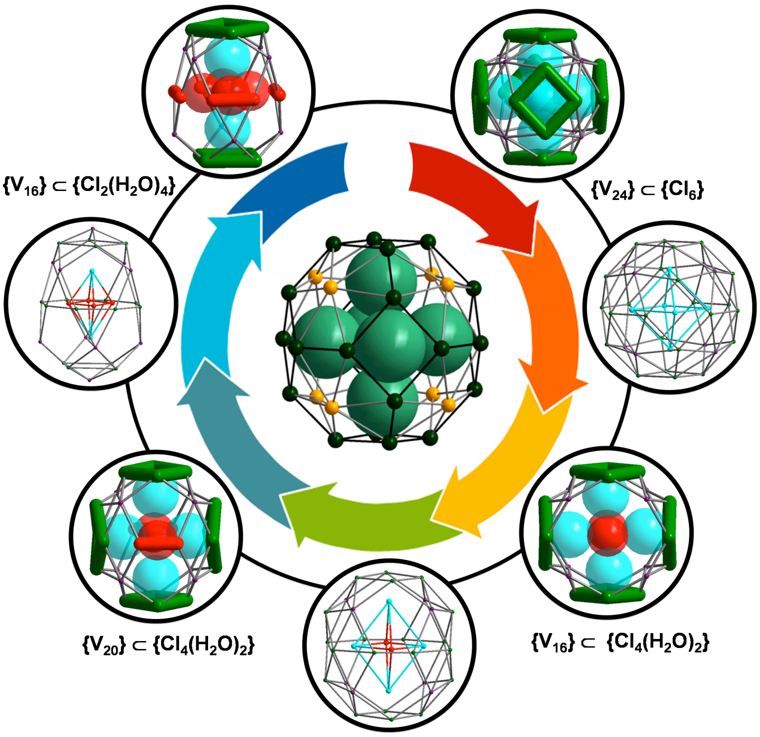

Fig. S9 Pictographical representation that highlights a comparable supramolecular anion effect in a polyoxovanadate system. In contrast to the discussed Mn system, here halide templates reside in the cavities of hollow cluster cages; in this system chloride ions stabilize tetranuclear vanadate $\{V_4\}$ units (represented as green squares) and H_2O molecules stabilize dinuclear $\{V_2\}$ sub-units (represented as red lines); see also *J. Am. Chem. Soc.* ***2011***, *133, 11240*.